THE JOURNAL OF BIOLOGICAL CHEMISTRY VOL. 290, NO. 15, pp. 9511–9520, April 10, 2015
Published in the U.S.A.

LINGO-1 Protein Interacts with the p75 Neurotrophin Receptor in Intracellular Membrane Compartments*

Received for publication, August 27, 2014, and in revised form, January 26, 2015 Published, JBC Papers in Press, February 9, 2015, DOI 10.1074/jbc.M114.608018

James S. Meabon[‡§], Rian De Laat[¶], Katsuaki Ieguchi[‖], Jesse C. Wiley[**], Mark P. Hudson[‡‡], and Mark Bothwell[‡‡1]

From the Departments of [‡]Psychiatry and Behavioral Sciences, [**]Comparative Medicine, and [‡‡]Physiology and Biophysics, University of Washington, Seattle, Washington 98195, the [§]Mental Illness Research Education and Clinical Center, Veterans Affairs Medical Center, Seattle, Washington 98108, [¶]Immusoft, Seattle, Washington 98103, and the [‖]Department of Pharmacology, Tokyo Women's Medical University, Tokyo 162-8666, Japan

Background: LINGO-1·p75^{NTR}·NgR complexes at the cell surface are believed to mediate responses to myelin inhibitors of axon growth.
Results: LINGO-1 is intracellular and competes with NgR for binding to p75^{NTR}.
Conclusion: The existence of cell-surface ternary complexes of p75^{NTR}, NgR, and LINGO-1 cannot be confirmed.
Significance: The commonly accepted mechanism for p75^{NTR}-mediated responses of axons to inhibitory myelin proteins is untenable.

Axon outgrowth inhibition in response to trauma is thought to be mediated via the binding of myelin-associated inhibitory factors (*e.g.* Nogo-66, myelin-associated glycoprotein, oligodendrocyte myelin glycoprotein, and myelin basic protein) to a putative tripartite LINGO-1·p75^{NTR}·Nogo-66 receptor (NgR) complex at the cell surface. We found that endogenous LINGO-1 expression in neurons in the cortex and cerebellum is intracellular. Mutation or truncation of the highly conserved LINGO-1 C terminus altered this intracellular localization, causing poor intracellular retention and increased plasma membrane expression. p75^{NTR} associated predominantly with natively expressed LINGO-1 containing immature *N*-glycans, characteristic of protein that has not completed *trans*-Golgi-mediated processing, whereas mutant forms of LINGO-1 with enhanced plasma membrane expression did not associate with p75^{NTR}. Co-immunoprecipitation experiments demonstrated that LINGO-1 and NgR competed for binding to p75^{NTR} in a manner that is difficult to reconcile with the existence of a LINGO-1·p75^{NTR}·NgR ternary complex. These findings contradict models postulating functional LINGO-1·p75^{NTR}·NgR complexes in the plasma membrane.

LINGO-1 (leucine-rich repeat Ig domain-containing Nogo-interacting protein 1) was originally identified as an essential component of a cell-surface receptor complex mediating axon growth cone collapse in response to certain membrane proteins of CNS myelin (1). These myelin-associated inhibitory factors (MAIFs),[2] including Nogo-A, myelin-associated glycoprotein, and oligodendrocyte myelin glycoprotein, have been implicated in restricting the regeneration of axons following CNS injuries in mammals. The Nogo-66 receptor (NgR) binds all three of these structurally dissimilar MAIFs (2, 3). NgR is a glycosylphosphatidylinositol-linked membrane protein. Lacking a transmembrane or intracellular domain (ICD), NgR must associate with other membrane proteins to propagate an intracellular signal. Two members of the TNF receptor superfamily, p75^{NTR} (p75 neurotrophin receptor) and Troy, function interchangeably as co-receptors for NgR-dependent activation of RhoA, which mediates repellant effects of MAIFs on axon growth cones (4).

The observation that coexpression of p75^{NTR} and NgR in COS-7 cells is insufficient to generate MAIF-dependent activation of RhoA led to the discovery of LINGO-1 as a third essential component of the functional receptor complex (1). This study suggested that MAIF-dependent inhibition of axon growth is mediated by a cell-surface receptor consisting of a ternary complex of p75^{NTR}, NgR, and LINGO-1. Other functions have been attributed to LINGO-1, including inhibition of oligodendrocyte differentiation (5–7), negative regulation of EGF receptor signaling (8), control of proliferation and differentiation of neural progenitor cells (9), and regulation of amyloidogenic processing of the β-amyloid precursor protein (10). All of these actions have been attributed to LINGO-1 in the plasma membrane, as these functions are inhibited by exposure of cells to the extracellular domain of LINGO-1 fused to the immunoglobulin Fc domain and/or by exposure of cells to an antibody against LINGO-1. Reflecting the perceived importance of expression of LINGO-1 at the cell surface, *in vitro* mutagenesis has been employed to characterize sites of *N*-glycosylation that are required for trafficking of LINGO-1 through the secretory pathway to the cell surface (11).

We investigated the nature of the functional collaboration of LINGO-1 with p75^{NTR} and NgR. These studies led to the discovery that little (if any) LINGO-1 is expressed at the cell surface. Our evidence indicates that LINGO-1 is localized predominantly to membranes of the biosynthetic secretory

* This work was supported, in whole or in part, by National Institutes of Health Grant NS47348 (to M. B.).
[1] To whom correspondence should be addressed: Dept. of Physiology and Biophysics and Inst. for Stem Cell and Regenerative Medicine, University of Washington, Seattle, WA 98109. Tel.: 206-543-7924; Fax: 206-543-0934; E-mail: mab@uw.edu.
[2] The abbreviations used are: MAIF, myelin-associated inhibitory factor; NgR, Nogo-66 receptor; ICD, intracellular domain; WGA, wheat germ agglutinin; β-COP, β-coatomer protein; HMM, high molecular mass; LMM, low molecular mass.

pathway and to membranes of the endocytic system. Restriction of trafficking of LINGO-1 to the cell surface is mediated by highly conserved sequences in its short ICD. We discuss how these features of LINGO-1 function may impact $p75^{NTR}$-mediated signaling by MAIFs.

EXPERIMENTAL PROCEDURES

Plasmid Constructs—A eukaryotic expression plasmid for full-length human LINGO-1 (IMAGE:4214343) was purchased from Thermo Scientific Open Biosystems. N-terminal preprotrypsin/FLAG-tagged human LINGO-1 lacking the native secretion signal (FLAG-LINGO-1) was created using standard molecular biology techniques with oligonucleotides 5′-CACAAGCTTTGCCCGCCCCG-3 and 5′-CACTCTAGATCATATCATCTTCATGTTGAACTTGCGG-3′ and pFLAG-CMV-1 (Sigma). A C-terminal V5-His_6 epitope fusion to human LINGO-1 (LINGO-1-V5) and LINGO-1 missing the prospective ICD (LINGO-1-ΔICD-V5) were created with PCR-generated DNA fragments using forward oligonucleotide primer 5′-CACCATGCAGGTGAGCAAGAGG-3′ and reverse primers 5′-TATCATCTTCATGTTGAACTTGCG-3′ and 5′-GTTGCCCTTGCCCCGGCTCCA-3′, respectively, and a pcDNA3.1 directional TOPO expression kit (Invitrogen) according to the manufacturer's instructions. All oligonucleotides were purchased from Integrated DNA Technologies. $p75^{NTR}$ constructs were a gift from Moses Chao, and NgR-FLAG was a gift from K. Wang and Z. He.

Cell Culture, Transfection, and Treatments—HEK293 cells were routinely cultured in pH 7.2 DMEM (Mediatech) containing 10% fetal bovine serum (HyClone) and 1% penicillin/streptomycin (Mediatech) at 37 °C and 5% CO_2. Unless indicated otherwise, cells were plated at 30–50% confluency in 6-well plates 20–24 h prior to transient transfection and transfected using Lipofectamine 2000 (2.5 μl/μg of DNA; Invitrogen) and 1 μg (unless indicated otherwise) of plasmid DNA/construct transfected in DMEM containing 10% fetal bovine serum without antibiotics. Cells were harvested 24 h post-transfection. Immunoprecipitants were treated with endoglycosidase H (Calbiochem) according to the manufacturer's protocol. MitoTracker Red CM-H_2XRos (Molecular Probes) was used as recommended by the manufacturer. In some experiments, Alexa Fluor 555-conjugated wheat germ agglutinin (WGA) or fluorescently conjugated phalloidin (Molecular Probes) was used according to the manufacturer's protocol for labeling pre-fixed eukaryotic cells. Human breast cancer cell lines HCC1937, MDA-MB-231, and MCF-7 were obtained from Dr. Mary-Claire King (University of Washington).

Immunoprecipitation, Gel Electrophoresis, and Immunoblot Analysis—Cells cultured in 6-well format were washed twice with ice-cold PBS (2.67 mM potassium chloride, 1.47 mM monobasic potassium phosphate, 138 mM sodium chloride, and 8.1 mM dibasic sodium phosphate, pH 7.4). Ice-cold cell homogenization buffer (20 mM Tris, pH 7.6, 1 mM EDTA, 0.5 mM EGTA, 1% Triton X-100, and 250 mM sucrose) was supplemented with protease inhibitor mixture for mammalian tissues (Sigma). Lysates were centrifuged at 16,000 × *g* for 20 min, a small aliquot was removed for protein quantitation by BCA (Pierce), and samples were either placed in sample loading buffer containing SDS and 2% β-mercaptoethanol or immunoprecipitated with the appropriate antibody. Immunoprecipitations were performed by incubating 90 μl of cleared cell lysate with 1 μg of primary antibody and 250 μl of simple immunoprecipitation wash buffer (10 mM Tris, pH 7.5, 150 mM NaCl, 0.1% (v/v) Triton X-100, and 5% (v/v) glycerol) overnight at 4 °C with gentle agitation, after which 25 μl of a 50% slurry of protein A-Sepharose CL-4B (GE Healthcare) was added and further incubated for 1 h. Sepharose beads were then washed three times with 0.5 ml of ice-cold simple immunoprecipitation wash buffer. The final wash was removed, 20 μl of 1.5× SDS sample loading buffer (94 mM Tris, pH 6.8, 3.0% (w/v) SDS, 0.03% (w/v) bromphenol blue, 15% (v/v) glycerol, and 3% (v/v) 2-mercaptoethanol) was added, and the samples boiled for 5 min. All samples were separated on Ready Gel or Criterion (18-well) Tris-HCl precast 4–20% acrylamide gel (Bio-Rad) following the manufacturer's recommendations, and SDS-PAGE and immunoblotting were performed as described previously (12). For immunoprecipitation from primary tissues, brains were harvested from decapitated postnatal day 0 mouse pups. Dissection was performed in ice-cold PBS, pH 7.4, and collected tissues were kept on ice until lysis in cell homogenization buffer.

Biotinylation of Cell-surface Proteins—At ~24 h post-transfection, cells were rinsed three to five times with ice-cold PBS, pH 8.0, and left to stabilize for 15–30 min at 4 °C. EZ-Link sulfo-NHS-LC-biotin (Pierce), freshly prepared at 2 mg/ml in ice-cold PBS, pH 8.0, was added to each well, and culture dishes were incubated on ice at 4 °C for 30 min. Cells were then rinsed three to five times with PBS and 100 mM glycine, incubated at 4 °C for 5 min in the final rinse, lysed in cell homogenization buffer, and immunoprecipitated with ImmunoPure-immobilized streptavidin beads (50 μl/lysates; Pierce). For experiments employing biotinylation to identify cell surface proteins of cortical neurons, as a control to demonstrate the capacity of intracellular proteins to be biotinylated, cultures were briefly exposed to the biotinylation reagent after permeabilization in PBS/0.1% saponin.

Primary Culture—C57BL/6 postnatal day 0 mouse pup brains were removed and dissociated as described previously (14). Purified neural cultures were plated at 1.25×10^5 to 2.5×10^5 cells/18 mm on glass coverslips coated with poly-D-lysine (0.1 mg/ml in distilled H_2O; Sigma) and allowed to grow for 5–7 days in complete Neurobasal A medium (Invitrogen). The medium was not changed during the course of incubation. For studies of cellular distribution of LINGO in heart cells, dissociated cardiac myocytes were prepared as described previously (14).

Immunocytochemistry—Coverslip-grown cultures were rinsed with PBS, pH 7.4, and fixed with 4% (w/v) paraformaldehyde in PBS for 30 min. Coverslips were then rinsed with PBS and permeabilized with 0.25% (v/v) Triton X-100 in PBS for 15 min. Permeabilization was followed by another PBS rinse. Coverslips were then blocked with 10% (w/v) BSA in PBS for 15 min and incubated overnight at 4 °C in primary antibody mixtures. The following primary antibodies were used: rabbit anti-LINGO-1 (1:1000; Upstate), mouse anti-LINGO-1 (1:500; R&D Systems), mouse anti-FLAG (1:1000; Sigma), mouse anti-V5 (1:1000; Invitrogen), mouse anti-c-Myc (1:500) (12), mouse anti-EEA1 (1:500; BD Transduction Laboratories), mouse anti-

Rab11 (1:500; Millipore), mouse anti-Rab7 (1:500; Sigma), mouse anti-Rab5 (1:250; Santa Cruz Biotechnology), mouse anti-GM130 (1:500; Abcam), mouse anti-mannose 6-phosphate receptor (1:1000; Abcam), mouse anti-β-coatomer protein (β-COP; 1:2000; Sigma), and goat anti-LAMP2 (1:200; Santa Cruz Biotechnology). After incubation, the primary antibodies were removed, and coverslips were rinsed three times with PBS (once quickly and twice for 10 min each). Coverslips were then incubated for 3 h at 4 °C with the appropriate secondary reagents (Molecular Probes): Alexa Fluor 568-conjugated donkey anti-goat IgG (1:1000), Alexa Fluor 555-conjugated donkey anti-rabbit IgG (1:1000), Alexa Fluor 568-conjugated donkey anti-mouse IgG (1:1000), Alexa Fluor 488-conjugated donkey anti-rabbit IgG (1:1000), and/or Alexa Fluor 546-conjugated streptavidin (1:2000). Coverslips were washed six times with cold PBS (three times quickly and three times for 10 min each), incubated with Hoechst 33258 (1:20,000) in distilled H_2O for 7 min, post-fixed with 4% paraformaldehyde for 10 min, rinsed with PBS, and washed twice for 10 min with distilled H_2O. Coverslips were mounted onto slides with 1:1 glycerol/distilled H_2O (plus 0.01% thimerosal, final concentration). All primary and secondary antibody mixtures were in 2.5% BSA in PBS.

Confocal Microscopy—Fixed cells were imaged using a Zeiss LSM 510 META confocal microscope. 405 nm diode, 488 nm argon, and 543 HeNe excitation lasers were used. Images were routinely acquired at a depth yielding maximum fluorophore signals throughout the highest amount of neurite arborization resolvable. Only healthy-appearing cells with normal morphology and non-pyknotic nuclei were imaged. In studies using cells transfected with LINGO-1 plasmid, we used the smallest concentration of construct that would achieve readily detectable levels of LINGO-1 immunoreactivity to avoid possible effects of overexpression on intracellular trafficking of LINGO-1. Images were obtained at ×40 or ×63 (oil immersion) in multitrack multiframe mode with line averaging (set to 4). For co-localization studies, images were analyzed with the Imaris (Bitplane) co-localization plug-in and two-channel thresholding held constant within image sets to measure the percent region of interest co-localized between LINGO and the queried markers. The mean percent region of interest co-localization values obtained for all images were then determined using Microsoft Excel.

Clustal Alignment—AlignX (Vector NTI, Invitrogen), which uses a modified ClustalW algorithm, was employed for alignment of LINGO-1 sequences according to the developer's suggestions and parameters using mouse LINGO-1 (NP_851419.1) as a reference sequence for comparison with human (NP_116197.4), chicken (NP_001019748.1), *Xenopus* (NP_001093719.1), and elephant shark (AAVX01545473.1) LINGO-1 sequences.

RESULTS

LINGO Is Not Observed at the Plasma Membrane—Cultured cerebellar granule neurons represent one system in which LINGO-1-dependent MAIF-induced neurite outgrowth inhibition has been reported (1). We characterized the distribution of LINGO-1 immunoreactivity by immunofluorescence confocal microscopy of dissociated cerebellar granular neurons from neonatal mice. The antibody we used reacts equally well with LINGO-1, LINGO-2, and LINGO-3 (data not shown); hence, we will hereafter refer to the protein identified generically as LINGO unless the identity of the LINGO paralog responsible was identified. To clearly delineate the plasma membrane, membrane proteins were covalently labeled with biotin by exposure to the membrane-impermeant reagent sulfo-NHS-LC-biotin, and biotin distribution was revealed by reaction with fluorescently labeled streptavidin. To our surprise, we could not detect LINGO immunoreactivity at the plasma membrane (Fig. 1*A*). Instead, LINGO immunoreactivity was observed as intracellular puncta, presumably representing intracellular membrane vesicles. This finding is consistent with a previous study that showed abundant intracellular localization of LINGO-1 immunoreactivity in differentiating neural stem cells (9).

To assess whether a similar intracellular distribution characterizes other types of neurons, we localized LINGO-1 in neonatal mouse cortical neurons by immunofluorescence microscopy, as LINGO-1 is highly expressed in the developing mouse cortex (15). For this study, we used an antibody against the extracellular domain of LINGO-1, as this epitope should be accessible to antibody in intact non-permeabilized cells only if it is expressed in the plasma membrane. LINGO-1 immunoreactivity was not detected in non-permeabilized cells, but was detected in intracellular puncta, presumably representing intracellular membranes, in detergent-permeabilized cells (Fig. 1*B*). As an alternative approach to assess whether LINGO-1 is expressed at the cell surface, we examined the ability of the membrane-impermeant reagent sulfo-NHS-LC-biotin to biotinylate LINGO-1 in cultured neonatal mouse cortical neurons. Biotinylation was performed either with intact viable cells or after permeabilization of cells by exposure to 0.1% saponin. Following biotinylation, cells were washed and then solubilized in Triton X-100-containing buffer. Biotinylated proteins were isolated by precipitation with streptavidin-coated beads and resolved by SDS-PAGE, after which the quantity of several proteins, including LINGO, was assessed by immunoblot analysis. Immunoreactive Trk neurotrophin receptor protein (a mixture of TrkB and TrkC in cortical neurons) was used as a representative protein that distributes in both plasma membrane and intracellular membrane compartments, whereas pyruvate kinase was used as marker of the cytoplasmic compartment. Fig. 1*C* shows that for cells biotinylated after permeabilization, the biotin-containing fraction of protein contained pyruvate kinase, Trk, and LINGO-1. However, when cells were biotinylated without prior permeabilization, the biotinylated fraction of protein contained Trk, but not pyruvate kinase or LINGO. Thus, LINGO behaved as an exclusively intracellular protein in biotinylation experiments.

Although LINGO-1 is most highly expressed in neural tissue, other tissues express one or more of the LINGO paralogs. We performed LINGO immunoprecipitation followed by immunoblot analysis to survey several mouse tissues for LINGO expression, as illustrated in Fig. 1*D*. Consistent with previously published studies, we found that LINGO expression was higher in neural tissues than in non-neural tissues, but significant LINGO immunoreactivity was present in a few non-neural tis-

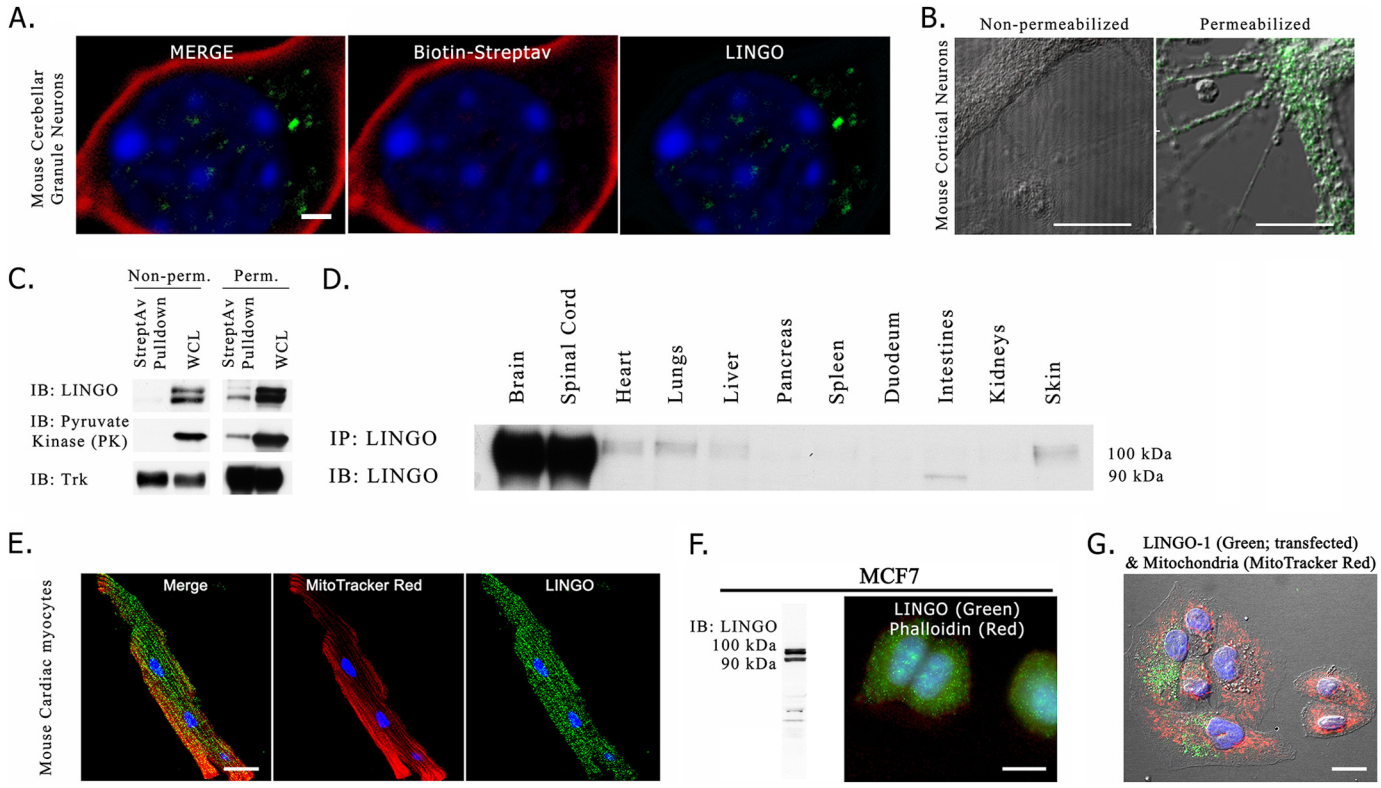

FIGURE 1. **Intracellular localization of LINGO-1.** *A*, confocal fluorescence microscopic image of the soma of a single cultured mouse cerebellar granule neuron following covalent labeling of plasma membrane proteins with biotin. Cultured cerebellar granule neurons were exposed to sulfo-NHS-LC-biotin and washed, after which biotin was localized by reaction with fluorescently labeled streptavidin (*Streptav*), and LINGO-1 was localized by indirect immunofluorescence. The image is a *z*-stack maximum intensity projection. DAPI-stained nuclear chromatin (*blue*) was distributed as foci of condensed chromatin distributed through the nucleus, which fills much of the volume of the soma. Streptavidin-labeled biotin (*red*) did not co-localize with immunofluorescently labeled LINGO-1 (*green*), which was observed as intracellular puncta. Focusing through the *z*-series indicated that the LINGO-1 immunoreactive puncta were distributed above and below the nucleus (not shown). *B*, cultured neonatal mouse cortical neurons imaged by phase contrast and immunofluorescence. Cells were immunostained with antibody against the extracellular domain of LINGO-1 (*green*) either for non-permeabilized cells (*left panel*) or for cells in which the outer membrane was permeabilized by exposure to buffer containing 0.1% saponin (*right panel*). *C*, immunoblot (*IB*) results of streptavidin bead pulldown assay with non-permeabilized (*Non-perm.*) or saponin-permeabilized (*Perm.*) biotinylated dissociated mouse neuronal cultures. In non-permeabilized cultures, neither LINGO-1 nor the cytoplasmic protein pyruvate kinase was present in the precipitated cell-surface biotinylated protein fraction, whereas the cell surface-expressed transmembrane protein Trk was present in the precipitated cell-surface biotinylated protein fraction. In cultures briefly permeabilized with 0.1% saponin, biotinylation of LINGO and intracellular proteins was observed, demonstrating that the lack of LINGO pulldown with streptavidin was not due to non-reactivity of LINGO with sulfo-NHS-LC-biotin. *WCL*, whole cell lysate. *D*, anti-LINGO immunoblot of mouse tissue lysates reveals LINGO protein expression in heart, lungs, liver, and skin, as well as brain and spinal cord. *IP*, immunoprecipitation. *E*, intracellular localization of LINGO in cultured mouse cardiac cells. Live cultured cardiac myocytes were loaded with MitoTracker Red CM-H_2XRos (used as an intracellular label), fixed, immunostained for LINGO (*green*), and imaged by confocal microscopy. The image is a maximum intensity projection. LINGO immunoreactive puncta were distributed among mitochondria in the cell's interior. *F*, intracellular localization in a human breast carcinoma cell line. *Left panel*, anti-LINGO immunoblot showing LINGO expression in the MCF-7 cell line. *Right panel*, immunofluorescence microscopy of LINGO distribution in MCF-7 cells. Cells were labeled with DAPI (*blue*) to reveal nuclei, fluorescently conjugated phalloidin (*red*) to label the prominent F-actin matrix lining the cell surface, and anti-LINGO antibody (*green*). LINGO immunoreactivity was localized to intracellular puncta. *G*, intracellular localization of LINGO-1 immunoreactivity in HeLa cells transiently transfected with human wild-type LINGO-1 expression plasmid. Mitochondria were stained with MitoTracker Red as an intracellular marker. Nuclear chromatin was stained with DAPI (*blue*). LINGO-1 immunofluorescence is shown in *green* . *Scale bars* = 1 μm (*A*) and 10 μm (*B* and *E–G*) .

sues, including heart and lung. To determine whether LINGO proteins are restricted to intracellular membranes in non-neural cells as they are in neurons, we examined the subcellular distribution of LINGO in cultured mouse cardiac cells by immunofluorescence microscopy using mitochondria as a marker of the cytoplasmic compartment. As shown in Fig. 1*E*, LINGO immunoreactivity was abundantly present as intracellular puncta, whereas no cell-surface LINGO immunoreactivity was apparent.

As the immunoblot analysis shown in Fig. 1*D* revealed that LINGO is expressed in several epithelial tissues such as skin and lung, we performed immunofluorescence microscopy and immunoblot analysis to screen several human epithelial cell lines, and we identified three human breast carcinoma cell lines (MCF-7, HCC1937, and MDA-MB-231) that express LINGO. We examined LINGO subcellular distribution in these cell lines by immunofluorescence microscopy. The results for MCF-7 cells are shown in Fig. 1*F*. LINGO was present as intracellular puncta, presumably reflecting expression on intracellular membranous organelles, whereas no LINGO could be detected at the cell surface.

Because of the uncertainty concerning whether these results reflected LINGO-1 or another LINGO paralog, we assessed the expression of LINGO-1 in cultured human epithelial cells by transfecting an epithelial cell line that normally lacks LINGO immunoreactivity (HeLa cells) with LINGO-1 plasmid. In these experiments, we adjusted the quantity of LINGO-1 plasmid transfected to avoid expressing LINGO-1 at levels higher than those observed in cell types that natively express LINGO proteins. As shown in Fig. 1*G*, we again found that LINGO-1 was

localized as intracellular puncta, and there was no evidence for LINGO-1 at the plasma membrane.

Conserved C-terminal Residues of the LINGO-1 ICD Are Essential for Intracellular Localization—The extracellular domains of LINGO family members share several structural motifs, including a series of leucine-rich repeat motifs (which are flanked by N- and C-terminal leucine-rich repeat cap variants) and an IgC2 domain proximal to the type 1 transmembrane domain. Clustal alignment of various vertebrate LINGO-1 sequences revealed that the LINGO-1 ICD sequence has been highly conserved through evolution (Fig. 2*A*), suggesting that this sequence is functionally important. ICDs of membrane proteins commonly bind cytoplasmic proteins that control trafficking between membrane subcompartments. Because the ICD of LINGO-1 is quite short, any alteration of this sequence is likely to impact LINGO-1 trafficking. Several previous studies demonstrating expression of LINGO-1 in the plasma membrane relied on overexpression of LINGO-1 constructs bearing C-terminal epitope tags. We reasoned that such modifications might disrupt the mechanisms that normally control intracellular trafficking of LINGO-1. To examine this possibility, we constructed plasmids encoding a series of LINGO-1 mutants (Fig. 2*B*) and compared the distribution of wild-type and mutant forms of LINGO-1 in transiently transfected HEK293 cells by confocal immunofluorescence microscopy (Fig. 2*C*). Untagged wild-type LINGO-1 was expressed as discrete microdomains, suggesting intracellular puncta. Because of our concern that protein binding might mask the antibody epitope in the C terminus of LINGO-1, we constructed N-terminal FLAG-tagged LINGO-1 (FLAG-LINGO-1). When stained with an anti-FLAG antibody, FLAG-LINGO-1 displayed punctum-like localization identical to that of wild-type LINGO-1. However, LINGO-1 altered by the addition of a C-terminal V5 tag (LINGO-1-V5) or by truncation of the C-terminal residues (LINGO-1-ΔICD-V5) was expressed in a lamellar distribution, suggesting close association with and potential insertion into the plasma membrane. WGA is a lectin that binds to sialic acid and *N*-acetylglucosaminyl residues found in the extracellular domains of membrane glycoproteins and is used to stain surface membranes. To extend the methods used to determine the relationship between these LINGO-1 constructs and the cell surface, we applied fluorescently conjugated WGA to briefly fixed HEK293 cells expressing wild-type LINGO-1 or LINGO-1-V5. Wild-type LINGO-1 was expressed in a punctate distribution in the interior part of the cell not labeled with WGA (Fig. 2*D*). However, LINGO-1-V5 co-localized extensively with the WGA-labeled cell surface. These results demonstrate that an intact and untagged LINGO-1 C terminus is essential for normal retention of LINGO-1 on intracellular membranes.

$p75^{NTR}$ Interacts Preferentially with LINGO-1 Isoforms That Have Not Completed Golgi-mediated Processing—Endogenously expressed LINGO-1 or LINGO-1 expressed from transfected plasmids appeared on immunoblots as two distinct bands, which we refer to as high molecular mass (HMM; ~100 kDa) and low molecular mass (LMM; ~90 kDa) LINGO-1 (Fig. 1*B*). Such heterogeneity in apparent molecular mass is commonly observed for membrane glycoproteins, which are typically modified by the addition of high-mannose core *N*-glycans in the endoplasmic reticulum, followed by modification of these *N*-glycans in the *cis*-Golgi. LINGO-1 is known to be modified by *N*-glycosylation (16). To test the hypothesis that LMM LINGO-1 might represent immature LINGO-1 that has not completed *trans*-Golgi-mediated processing of *N*-glycans, we exposed detergent extracts of HEK293 cells expressing LINGO-1 to endoglycosidase H, which deglycosylates proteins bearing immature high-mannose *N*-glycans, but does not deglycosylate proteins bearing mature post-Golgi *N*-glycans. Exposure of LINGO-1 to endoglycosidase H converted the 90-kDa LMM LINGO-1 species into a new 80-kDa species, presumably representing deglycosylated LINGO-1. In contrast, the HMM LINGO-1 species was much less affected, running as a slightly smaller and more diffuse band after exposure to endoglycosidase H (Fig. 3*A*), indicating that only a small fraction of the *N*-glycans on HMM LINGO-1 have a high-mannose structure. These results support the conclusion that HMM LINGO-1 represents the fully processed mature protein, whereas LMM LINGO-1 represents protein that has not completed Golgi-mediated processing. A caveat for this conclusion is that a few proteins have been reported to have *N*-glycans that escape Golgi-mediated conversion to the endoglycosidase H-resistant form as they traffic to the plasma membrane. Thus, we performed another experiment to address this issue.

A prediction of the hypothesis that LMM LINGO-1 represents protein that has not completed Golgi-mediated processing is that LMM LINGO-1 should not be detectable at the cell surface, even under conditions in which C-terminal mutations cause a significant amount of LINGO-1 to traffic to the cell surface. To test this prediction, we performed streptavidin pull-down assays with biotinylated cell-surface proteins from HEK293 cells expressing such mutant forms of LINGO-1. Consistent with our previous conclusions, HMM LINGO-1 was detected in the plasma membrane fraction, whereas LMM LINGO-1 was not (Fig. 3*B*).

A previous study carried out co-immunoprecipitation experiments to demonstrate complexes of LINGO-1 with NgR and $p75^{NTR}$ (1). If these complexes occur at the cell surface as part of a tripartite complex mediating MAIF-dependent signaling, one would expect that the mature form of LINGO-1 with fully processed *N*-glycans (HMM LINGO-1) would be preferentially incorporated into such complexes. To test this prediction, combinations of LINGO-1-V5, LINGO-1-ΔICD-V5, p75NTR-Myc, and FLAG-NgR were transiently overexpressed in HEK293 cells, and detergent lysates of cells were subsequently immunoprecipitated (Fig. 3*C*). Epitope tags were used in these studies to improve sensitivity for detection and to avoid the possibility that antibodies against native protein sequences would block protein domains mediating complex formation. Immunoprecipitation of NgR (via its FLAG epitope tag) resulted in a robust co-immunoprecipitation of both HMM LINGO-1 and LMM LINGO-1. However, only LMM LINGO-1 was co-immunoprecipitated with $p75^{NTR}$. This indicates that $p75^{NTR}$ forms complexes mainly with the fraction of LINGO-1 that has not completed trafficking through the *trans*-Golgi compartment. $p75^{NTR}$ did not associate to a detectable degree with mature post-Golgi LINGO-1 even under circumstances in

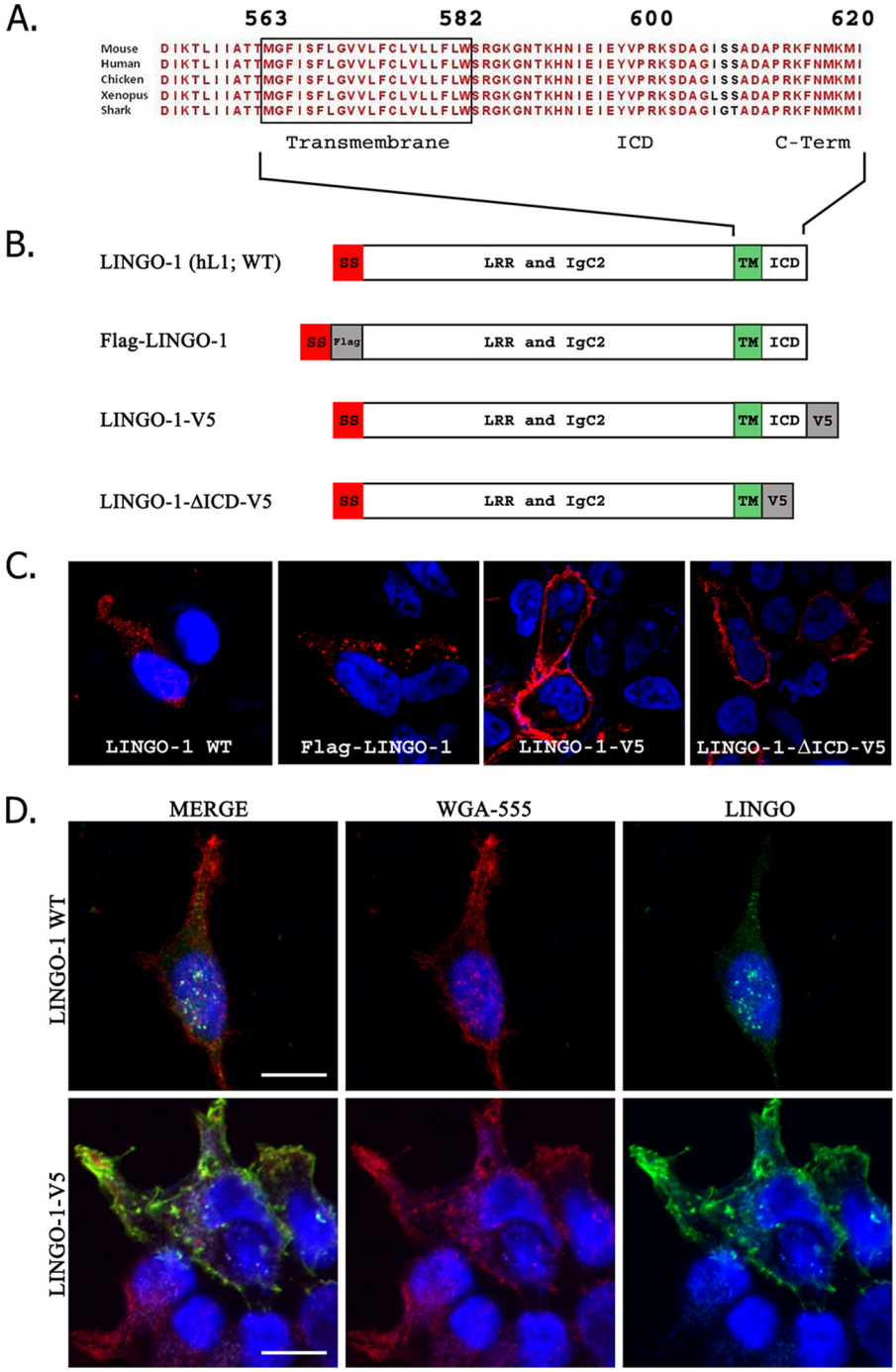

FIGURE 2. **The LINGO-1 C terminus is essential for proper subcellular localization.** *A*, illustration of the conservation of the LINGO-1 C terminus across vertebrate evolution. *B*, structure of various LINGO-1 constructs employed. *h*, human; *SS*, signal sequence; *LRR*, leucine-rich repeat; *TM*, transmembrane domain. *C*, subcellular distribution of wild-type (*WT*) and mutant LINGO-1 expressed in transiently transfected HEK293 cells imaged by confocal immunofluorescence microscopy. LINGO-1 detected by anti-LINGO, anti-FLAG, or anti-V5 antibody is shown in *red*. DAPI nuclear counterstain is shown in *blue*. Wild-type LINGO-1 or LINGO-1 bearing an N-terminal FLAG tag was expressed as apparent intracellular puncta, whereas LINGO-1 with an ICD deletion or bearing a C-terminal V5 tag trafficked to the cellular membrane. *D*, confocal immunofluorescence microscopy comparing distribution of LINGO-1 with distribution of lectin-labeled plasma membrane. HEK293 cells transiently transfected with LINGO-1 or LINGO-1 bearing a C-terminal V5 tag were briefly fixed and then reacted with fluorescently tagged Alexa Fluor 555-conjugated WGA (*red*), after which membranes were permeabilized by exposure to Triton X-100-containing buffer, and cells were immunostained with anti-LINGO-1 antibody (*green*). DAPI nuclear stain is shown in *blue*. LINGO-1-V5 co-localized extensively with Alexa Fluor 555-conjugated WGA-labeled plasma membrane, whereas LINGO-1 exhibited very little co-localization with Alexa Fluor 555-conjugated WGA. *Scale bars* = 10 μm.

which expression of LINGO-1 at the cell surface was artificially enhanced by deletion of C-terminal sequences that mediate intracellular retention.

To provide additional evidence concerning the membrane pools within which $p75^{NTR}$ and LINGO-1 interact, we localized these proteins in transfected HEK293 cells by confocal immunofluorescence microscopy. Consistent with our previous results, co-localization of $p75^{NTR}$ and LINGO-1 was observed only on intracellular puncta, but not at the cell surface (Fig. 3*D*). These results are not easily reconciled with the suggested par-

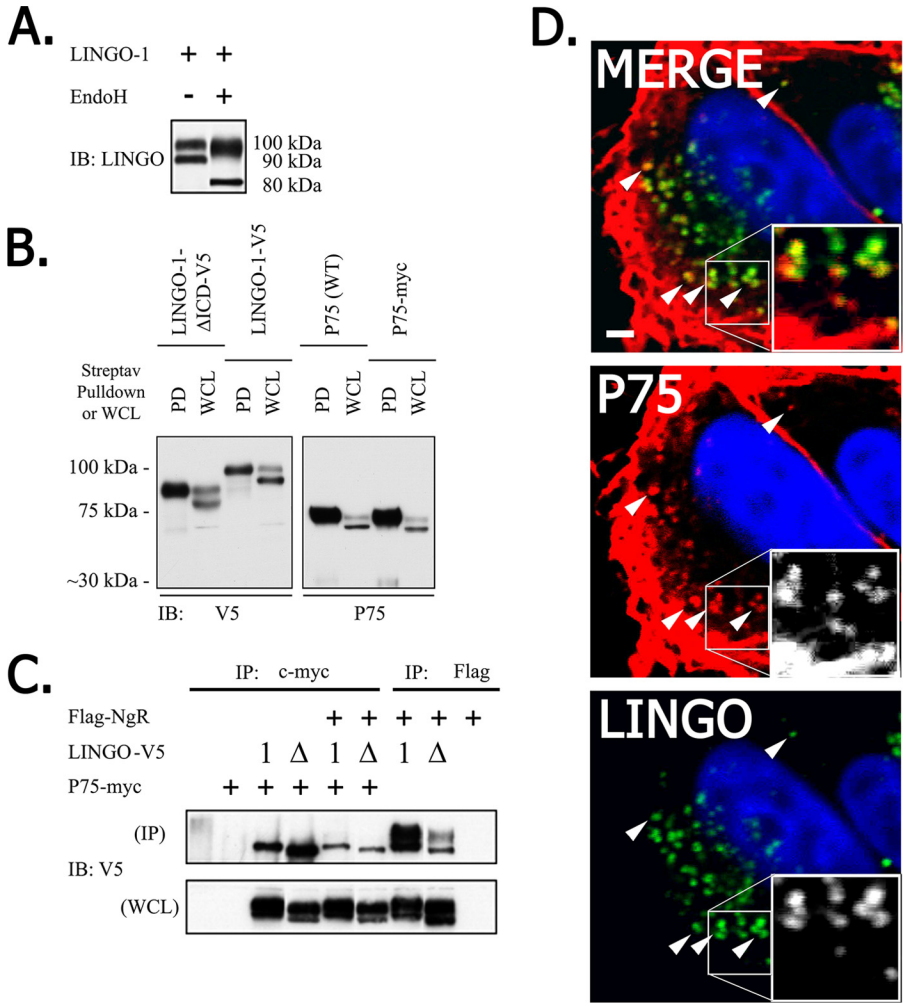

FIGURE 3. **p75^{NTR} interacts predominantly with intracellular LMM LINGO-1.** *A*, LMM LINGO-1 is selectively sensitive to endoglycosidase H (*EndoH*) activity. HEK293 cells were transiently transfected with LINGO-1 plasmid, LINGO-1 was immunoprecipitated, and immunoprecipitates were exposed to endoglycosidase H prior to immunoblot (*IB*) analysis. Endoglycosidase H exposure converted 90-kDa LMM LINGO-1 to an 80-kDa product, whereas 100-kDa HMM LINGO-1 exhibited only limited conversion to a slightly smaller form. *B*, only HMM LINGO-1 can traffic to the cell surface. HEK293 cells were transiently transfected with p75^{NTR} and C-terminal V5-tagged LINGO-1 or LINGO-1 with most of its ICD deleted, and cell-surface proteins were biotinylated. Cell-surface proteins isolated by streptavidin (*Streptav*) pulldown (*PD*) and total cell proteins (whole cell lysate (*WCL*)) were assessed by immunoblot analysis. Only HMM LINGO-1 species were detected in the surface-expressed fraction. No LMM LINGO-1 species were detected in the surface-expressed fraction. *C*, p75^{NTR} interacts exclusively with LMM LINGO-1. HEK293 cells were transiently transfected with plasmids encoding Myc-tagged p75^{NTR}, FLAG-tagged NgR, and V5-tagged LINGO-1 bearing wild-type or mutant C-terminal sequences. LINGO-1 in detergent extracts of cells was examined by immunoblot analysis with anti-V5 antibody either for whole cell lysates or following immunoprecipitation (*IP*) of NgR and p75^{NTR} with antibodies against FLAG and Myc epitope tags, respectively. NgR co-immunoprecipitated with both HMM LINGO-1 and LMM LINGO-1, whereas p75^{NTR} co-immunoprecipitated with only LMM LINGO-1. *D*, confocal immunofluorescence detection of p75^{NTR} (*red*) and LINGO-1 (*green*) co-localization in transfected HEK293 cells. LINGO-1·p75^{NTR} co-localization was restricted to intracellular puncta. Nuclei were stained with DAPI (*blue*).

ticipation of a tripartite LINGO-1·p75^{NTR}·NgR complex as a cell-surface MAIF receptor.

NgR Is Displaced from p75^{NTR} by LINGO-1—This experiment also revealed another unexpected result. Expression of NgR reduced the amount of LINGO-1 that co-immunoprecipitated with p75^{NTR} (Fig. 3*C*). This suggests that NgR and LINGO-1 compete for binding to p75^{NTR}. To examine this effect more systematically, we assessed the extent of p75^{NTR}·NgR complex formation over a range of levels of LINGO-1 expression. We observed that increasing LINGO-1 expression reduced the association of NgR with p75^{NTR} in a LINGO-1 dose-dependent manner (Fig. 4). (In this experiment, the condition representing the highest level of LINGO-1 expression achieved was uninformative concerning effects on avidity of NgR/p75^{NTR} association because the total levels of NgR and p75^{NTR} expressed were reduced.) The competition between NgR and LINGO-1 in binding p75^{NTR} is a scenario that is hard to reconcile with models postulating functional tripartite LINGO-1·p75^{NTR}·NgR complexes.

Identification of Intracellular Loci of LINGO-1 Expression—Because LINGO-1 apparently functions intracellularly, the identity of intracellular puncta containing LINGO-1 is of interest. We previously demonstrated that LINGO-1 down-regulates expression of several receptor tyrosine kinases, including TrkA, in a manner similar to the effect of a structurally related protein, LRIG1 (17). LRIG1 down-regulates several receptor tyrosine kinases by promoting endocytosis and lysosomal degradation (reviewed in Ref. 18). LINGO-1 has been reported to down-regulate EGF receptors by a mechanism involving enhanced endocytosis and lysosomal degradation of these

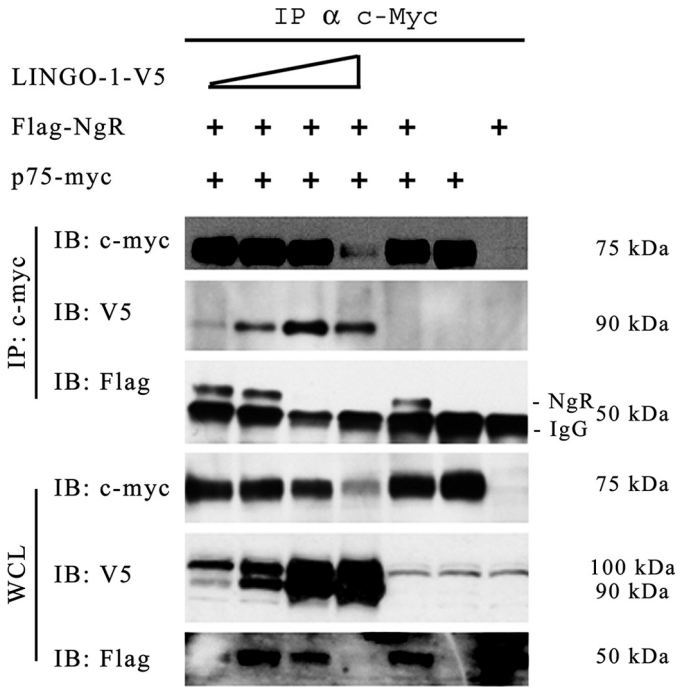

FIGURE 4. **Associative competition among putative tripartite LINGO-1·p75^{NTR}·NgR receptor members.** p75^{NTR} immunoprecipitation (*IP*) in the presence of increasing LINGO-1-V5 expression reduced the amount of co-immunoprecipitated NgR in a LINGO-1 dose-dependent manner. Epitope-tagged LINGO-1, p75^{NTR}, and NgR were expressed in transfected HEK293 cells. Cell extracts and immunoprecipitates made using antibody against the epitope tag of p75^{NTR} were assessed by immunoblot (*IB*) analysis using antibodies against the epitope tags of each protein. All lanes depicted derived from the same gel. For the anti-FLAG immunoblot of immunoprecipitates of FLAG-NgR, the prominent lower 50-kDa band is an artifact, representing the heavy chain of IgG. The band running slightly above the 50-kDa position represents FLAG-NgR. The first band in the last whole cell lysate (*WCL*) image (anti-FLAG) is partially obscured due to uneven blot transfer; NgR expression in this lane can be inferred by the strong co-immunoprecipitation of NgR via p75^{NTR}-Myc as seen in the upper blot.

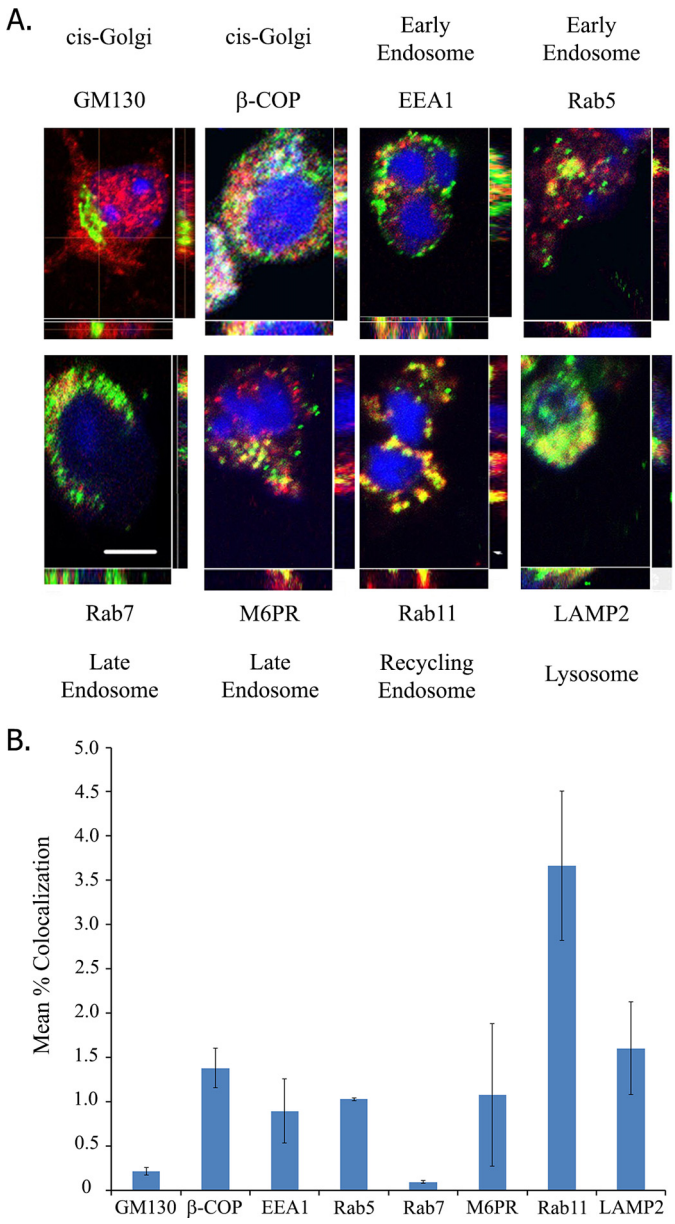

FIGURE 5. **Neuronal LINGO-1 localizes to subcellular membrane compartments of secretory and endocytic pathways.** *A*, confocal images of immunofluorescently stained LINGO-1 (*red*) and various membrane compartment markers (*green*) in cultured mouse cortical neurons. Images are maximum intensity projections with variation of density across orthogonal confocal image slices also depicted. Nuclei were stained with DAPI (*blue*). Membrane compartment markers include EEA1 (early endosomes), Rab5 (early endosomes), GM130 (*cis*-Golgi), β-COP (vesicles involved in anterograde and retrograde transport to/from the Golgi), mannose 6-phosphate receptor (*M6PR*; late endosomes), Rab7 (late endosomes), Rab11 (recycling endosomes), and LAMP2 (lysosomes). *Scale bar* = 10 μm. *B*, quantitation of LINGO co-localization with markers of various membrane compartments, assessed as percent of pixels displaying immunofluorescence signals for LINGO and each marker. Of the markers imaged, the greatest LINGO co-localization was observed with Rab11. Values are expressed as mean percent co-localization ± S.E. Rab11, $n = 197$ cells; GM130, $n = 52$ cells; β-COP, $n = 96$ cells; EEA1, $n = 266$ cells; Rab5, $n = 343$ cells; Rab7, $n = 39$ cells; mannose 6-phosphate receptor, $n = 138$ cells; LAMP2, $n = 106$ cells.

receptors (8). This suggests that LINGO-1 might be present in vesicles of the endosomal system. However, the observation that LINGO-1 interacts primarily with p75^{NTR} in a compartment of the secretory pathway earlier than the *trans*-Golgi implies that a pool of LINGO-1 resides in the secretory pathway. Consequently, we assessed the extent of co-localization of LINGO immunoreactivity with markers for various intracellular membrane compartments of the secretory and endocytic pathways in cultured cortical neurons by confocal immunofluorescence microscopy (Fig. 5, *A* and *B*). We observed a small degree of co-localization of LINGO-1 with markers of compartments within the secretory pathway, including β-COP (*cis*-Golgi/rough endoplasmic reticulum transit vesicles) and GM130 (*cis*-Golgi), and with markers of compartments of the endocytic pathway, including EEA1 (early endosomes), Rab5 (early endosomes), Rab7 (late endosomes), mannose 6-phosphate receptor (late endosomes), Rab11 (recycling endosomes), and LAMP2 (lysosomes). The greatest degree of overlap was observed for Rab11.

DISCUSSION

Our findings are difficult to reconcile with the widely accepted model that MAIF-dependent signaling is mediated by a ternary cell-surface complex of LINGO-1 and NgR with p75^{NTR} (1, 9, 19) or Troy (4, 20). The first result of our data that is inconsistent with this model is that we found native endogenously expressed LINGO-1 to be present exclusively on intracellular membranous structures. We found that modification of the LINGO-1 C terminus by deletion mutations or fusion

with a C-terminal V5 tag displaced LINGO-1 from its normal intracellular sites of expression and caused it to be strongly expressed at the cell surface. However, even under such conditions in which LINGO-1 is artificially diverted to the plasma membrane, our data indicate that physical complexes of $p75^{NTR}$ and LINGO-1 are represented mainly by the subfraction of LINGO-1 that has not completed Golgi-mediated processing. It is noteworthy that a study describing the importance of particular *N*-glycans for cell-surface expression of LINGO-1 used C-terminally modified forms of LINGO-1 exclusively (11). In disagreement with our findings, one report has described labeling of LINGO-1 by a cell-impermeant biotinylating reagent (10). Significantly, these investigators demonstrated biotinylation of LMM LINGO-1, a form that represents protein that has not completed Golgi-mediated processing of *N*-glycans, according to our results. This suggests that the reported biotinylation of LINGO-1 by a membrane-impermeant reagent reflects reaction of the reagent with LINGO-1 in intracellular compartments of the secretory pathway, possibly due to intracellular entry of the biotinylating reagent through the damaged plasma membrane.

Although we have been unable to detect LINGO-1 at the cell surface, the presence of LINGO-1 in membranes of the endocytic pathway suggests that LINGO-1 transiently visits the plasma membrane. This is not necessarily the case, however, as some membrane proteins traffic from the Golgi compartment directly to endosomes without visiting the cell surface (21).

The second result of our data that is inconsistent with the view that MAIF-dependent signaling employs a cell-surface LINGO-1·$p75^{NTR}$·NgR ternary complex is that LINGO-1 and NgR appear to compete for binding with $p75^{NTR}$. NgR and LINGO-1 are structurally related, as both contain multiple leucine-rich repeat domains. Thus, it seems likely that the competition reflects interaction of NgR and LINGO-1 with the same $p75^{NTR}$-binding site. If both LINGO-1 and NgR interactions are required for $p75^{NTR}$-dependent MAIF signaling, this suggests that NgR and LINGO-1 interact with $p75^{NTR}$ sequentially rather than simultaneously. Because we found that NgR and $p75^{NTR}$ are expressed at the cell surface, whereas LINGO-1 is not, models may be considered in which MAIF induced endocytosis of $p75^{NTR}$·NgR complexes allows association of the complex with LINGO-1 within endosomes. A report that MAIF-dependent activation of RhoA by $p75^{NTR}$·NgR complexes requires γ-secretase-mediated release of the ICD of $p75^{NTR}$ (22) and a report that this processing event follows endocytosis of $p75^{NTR}$ (23) suggest the possibility that LINGO-1 may influence endosomal processing of $p75^{NTR}$. It has been reported that internalized $p75^{NTR}$ accumulates most abundantly in Rab11-positive recycling endosomes (24). Thus, our observation that LINGO-1 is localized most abundantly in Rab11-positive endosomes supports the hypothesis that $p75^{NTR}$ and LINGO-1 interact functionally in this endocytic compartment. Our failure to detect physical complexes of $p75^{NTR}$ with mature post-Golgi LINGO-1 might be explained if LINGO-1 binding to $p75^{NTR}$ in recycling endosomes leads immediately to proteolytic processing of $p75^{NTR}$. The nature of this functional interaction remains to be explored.

It has been reported that MAIF-dependent activation of RhoA is dependent on the association of the LINGO-1 ICD with the protein kinase WNK1 (25). The most commonly reported functions of members of the WNK family of protein kinases concern regulated trafficking of various membrane proteins in the secretory and/or endocytic pathway (26–32). Taken together with our findings, this suggests that WNK1 may be important for delivering components of this LINGO-1·$p75^{NTR}$·NgR signaling pathway to the correct endocytic compartments. WNK1 is unlikely to be the only cytoplasmic protein influencing trafficking of LINGO-1, however, as we found that fusion of GFP to the LINGO-1 C terminus, like a C-terminal V5 fusion, prevents expression of LINGO-1 in its normal intracellular membrane compartments (data not shown), whereas similarly modified LINGO-1 interacts normally with WNK1 (25). One class of C-terminal motifs influencing membrane protein trafficking that is destroyed by C-terminal extensions is the PDZ (PSD-95/discs large/zona occludens-1) domain ligand motif (33). Such motifs generally employ five or six C-terminal residues, with the last three C-terminal residues contributing most critically. The six C-terminal residues of LINGO family members are highly conserved over vertebrate evolution. Although the last three residues of this sequence do not conform precisely to any known naturally existing PDZ domain ligand motif, they are similar to an artificially produced sequence that binds class III PDZ domains (33). Thus, the possibility that the trafficking and function of LINGO-1 are dependent on the interaction with a protein containing a class III PDZ domain deserves investigation.

In summary, in this study, we have identified the evolutionarily conserved ICD of LINGO-1 as being critical for maintaining its normal retention within intracellular membrane compartments. Our evidence suggests that $p75^{NTR}$ functions sequentially in binary complexes with NgR and LINGO-1 and that the functional interaction between $p75^{NTR}$ and LINGO-1 occurs after internalized $p75^{NTR}$ enters recycling endosomes.

REFERENCES

1. Mi, S., Lee, X., Shao, Z., Thill, G., Ji, B., Relton, J., Levesque, M., Allaire, N., Perrin, S., Sands, B., Crowell, T., Cate, R. L., McCoy, J. M., and Pepinsky, R. B. (2004) LINGO-1 is a component of the Nogo-66 receptor/p75 signaling complex. *Nat. Neurosci.* **7,** 221–228
2. Fournier, A. E., GrandPré, T., and Strittmatter, S. M. (2001) Identification of a receptor mediating Nogo-66 inhibition of axonal regeneration. *Nature* **409,** 341–346
3. Liu, B. P., Fournier, A., GrandPré, T., and Strittmatter, S. M. (2002) Myelin-associated glycoprotein as a functional ligand for the Nogo-66 receptor. *Science* **297,** 1190–1193
4. Shao, Z., Browning, J. L., Lee, X., Scott, M. L., Shulga-Morskaya, S., Allaire, N., Thill, G., Levesque, M., Sah, D., McCoy, J. M., Murray, B., Jung, V., Pepinsky, R. B., and Mi, S. (2005) TAJ/TROY, an orphan TNF receptor family member, binds Nogo-66 receptor 1 and regulates axonal regeneration. *Neuron* **45,** 353–359
5. Mi, S., Miller, R. H., Lee, X., Scott, M. L., Shulag-Morskaya, S., Shao, Z., Chang, J., Thill, G., Levesque, M., Zhang, M., Hession, C., Sah, D., Trapp, B., He, Z., Jung, V., McCoy, J. M., and Pepinsky, R. B. (2005) LINGO-1 negatively regulates myelination by oligodendrocytes. *Nat. Neurosci.* **8,** 745–751
6. Lee, X., Yang, Z., Shao, Z., Rosenberg, S. S., Levesque, M., Pepinsky, R. B., Qiu, M., Miller, R. H., Chan, J. R., and Mi, S. (2007) NGF regulates the expression of axonal LINGO-1 to inhibit oligodendrocyte differentiation and myelination. *J. Neurosci.* **27,** 220–225

7. Jepson, S., Vought, B., Gross, C. H., Gan, L., Austen, D., Frantz, J. D., Zwahlen, J., Lowe, D., Markland, W., and Krauss, R. (2012) LINGO-1, a transmembrane signaling protein, inhibits oligodendrocyte differentiation and myelination through intercellular self-interactions. *J. Biol. Chem.* **287,** 22184–22195
8. Inoue, H., Lin, L., Lee, X., Shao, Z., Mendes, S., Snodgrass-Belt, P., Sweigard, H., Engber, T., Pepinsky, B., Yang, L., Beal, M. F., Mi, S., and Isacson, O. (2007) Inhibition of the leucine-rich repeat protein LINGO-1 enhances survival, structure, and function of dopaminergic neurons in Parkinson's disease models. *Proc. Natl. Acad. Sci. U.S.A.* **104,** 14430–14435
9. Lööv, C., Fernqvist, M., Walmsley, A., Marklund, N., and Erlandsson, A. (2012) Neutralization of LINGO-1 during *in vitro* differentiation of neural stem cells results in proliferation of immature neurons. *PLoS ONE* **7,** e29771
10. Bai, Y., Markham, K., Chen, F., Weerasekera, R., Watts, J., Horne, P., Wakutani, Y., Bagshaw, R., Mathews, P. M., Fraser, P. E., Westaway, D., St George-Hyslop, P., and Schmitt-Ulms, G. (2008) The *in vivo* brain interactome of the amyloid precursor protein. *Mol. Cell. Proteomics* **7,** 15–34
11. Zhong, X., Pocas, J., Liu, Y., Wu, P. W., Mosyak, L., Somers, W., and Kriz, R. (2009) Swift residue-screening identifies key *N*-glycosylated asparagines sufficient for surface expression of neuroglycoprotein Lingo-1. *FEBS Lett.* **583,** 1034–1038
12. Kanning, K. C., Hudson, M., Amieux, P. S., Wiley, J. C., Bothwell, M., and Schecterson, L. C. (2003) Proteolytic processing of the p75 neurotrophin receptor and two homologs generates C-terminal fragments with signaling capability. *J. Neurosci.* **23,** 5425–5436
13. Wong, S. T., Henley, J. R., Kanning, K. C., Huang, K. H., Bothwell, M., and Poo, M. M. (2002) A $p75^{NTR}$ and Nogo receptor complex mediates repulsive signaling by myelin-associated glycoprotein. *Nat. Neurosci.* **5,** 1302–1308
14. Dilly, K. W., Rossow, C. F., Votaw, V. S., Meabon, J. S., Cabarrus, J. L., and Santana, L. F. (2006) Mechanisms underlying variations in excitation-contraction coupling across the mouse left ventricular free wall. *J. Physiol.* **572,** 227–241
15. Carim-Todd, L., Escarceller, M., Estivill, X., and Sumoy, L. (2003) *LRRN6A/LERN1* (leucine-rich repeat neuronal protein 1), a novel gene with enriched expression in limbic system and neocortex. *Eur. J. Neurosci.* **18,** 3167–3182
16. Mosyak, L., Wood, A., Dwyer, B., Buddha, M., Johnson, M., Aulabaugh, A., Zhong, X., Presman, E., Benard, S., Kelleher, K., Wilhelm, J., Stahl, M. L., Kriz, R., Gao, Y., Cao, Z., Ling, H. P., Pangalos, M. N., Walsh, F. S., and Somers, W. S. (2006) The structure of the Lingo-1 ectodomain, a module implicated in central nervous system repair inhibition. *J. Biol. Chem.* **281,** 36378–36390
17. Mandai, K., Guo, T., St Hillaire, C., Meabon, J. S., Kanning, K. C., Bothwell, M., and Ginty, D. D. (2009) LIG family receptor tyrosine kinase-associated proteins modulate growth factor signals during neural development. *Neuron* **63,** 614–627
18. Rubin, C., Gur, G., and Yarden, Y. (2005) Negative regulation of receptor tyrosine kinases: unexpected links to c-Cbl and receptor ubiquitylation. *Cell Res.* **15,** 66–71
19. Bandtlow, C., and Dechant, G. (2004) From cell death to neuronal regeneration, effects of the p75 neurotrophin receptor depend on interactions with partner subunits. *Sci. STKE* 2004, pe24
20. Park, J. B., Yiu, G., Kaneko, S., Wang, J., Chang, J., He, X. L., Garcia, K. C., and He, Z. (2005) A TNF receptor family member, TROY, is a coreceptor with Nogo receptor in mediating the inhibitory activity of myelin inhibitors. *Neuron* **45,** 345–351
21. Gonzalez, A., and Rodriguez-Boulan, E. (2009) Clathrin and AP1B: key roles in basolateral trafficking through trans-endosomal routes. *FEBS Lett.* **583,** 3784–3795
22. Domeniconi, M., Zampieri, N., Spencer, T., Hilaire, M., Mellado, W., Chao, M. V., and Filbin, M. T. (2005) MAG induces regulated intramembrane proteolysis of the p75 neurotrophin receptor to inhibit neurite outgrowth. *Neuron* **46,** 849–855
23. Urra, S., Escudero, C. A., Ramos, P., Lisbona, F., Allende, E., Covarrubias, P., Parraguez, J. I., Zampieri, N., Chao, M. V., Annaert, W., and Bronfman, F. C. (2007) TrkA receptor activation by nerve growth factor induces shedding of the p75 neurotrophin receptor followed by endosomal γ-secretase-mediated release of the p75 intracellular domain. *J. Biol. Chem.* **282,** 7606–7615
24. Escudero, C. A., Lazo, O. M., Galleguillos, C., Parraguez, J. I., Lopez-Verrilli, M. A., Cabeza, C., Leon, L., Saeed, U., Retamal, C., Gonzalez, A., Marzolo, M. P., Carter, B. D., Court, F. A., and Bronfman, F. C. (2014) The p75 neurotrophin receptor evades the endolysosomal route in neuronal cells, favouring multivesicular bodies specialised for exosomal release. *J. Cell Sci.* **127,** 1966–1979
25. Zhang, Z., Xu, X., Zhang, Y., Zhou, J., Yu, Z., and He, C. (2009) LINGO-1 interacts with WNK1 to regulate Nogo-induced inhibition of neurite extension. *J. Biol. Chem.* **284,** 15717–15728
26. Lee, B. H., Min, X., Heise, C. J., Xu, B. E., Chen, S., Shu, H., Luby-Phelps, K., Goldsmith, E. J., and Cobb, M. H. (2004) WNK1 phosphorylates synaptotagmin 2 and modulates its membrane binding. *Mol. Cell* **15,** 741–751
27. Fu, Y., Subramanya, A., Rozansky, D., and Cohen, D. M. (2006) WNK kinases influence TRPV4 channel function and localization. *Am. J. Physiol. Renal Physiol.* **290,** F1305–F1314
28. Golbang, A. P., Cope, G., Hamad, A., Murthy, M., Liu, C. H., Cuthbert, A. W., and O'Shaughnessy, K. M. (2006) Regulation of the expression of the Na/Cl cotransporter by WNK4 and WNK1: evidence that accelerated dynamin-dependent endocytosis is not involved. *Am. J. Physiol. Renal Physiol.* **291,** F1369–F1376
29. Cope, G., Murthy, M., Golbang, A. P., Hamad, A., Liu, C. H., Cuthbert, A. W., and O'Shaughnessy, K. M. (2006) WNK1 affects surface expression of the ROMK potassium channel independent of WNK4. *J. Am. Soc. Nephrol.* **17,** 1867–1874
30. Jiang, Y., Cong, P., Williams, S. R., Zhang, W., Na, T., Ma, H. P., and Peng, J. B. (2008) WNK4 regulates the secretory pathway via which TRPV5 is targeted to the plasma membrane. *Biochem. Biophys. Res. Commun.* **375,** 225–229
31. Subramanya, A. R., Liu, J., Ellison, D. H., Wade, J. B., and Welling, P. A. (2009) WNK4 diverts the thiazide-sensitive NaCl cotransporter to the lysosome and stimulates AP-3 interaction. *J. Biol. Chem.* **284,** 18471–18480
32. Fang, L., Garuti, R., Kim, B. Y., Wade, J. B., and Welling, P. A. (2009) The ARH adaptor protein regulates endocytosis of the ROMK potassium secretory channel in mouse kidney. *J. Clin. Invest.* **119,** 3278–3289
33. Wiedemann, U., Boisguerin, P., Leben, R., Leitner, D., Krause, G., Moelling, K., Volkmer-Engert, R., and Oschkinat, H. (2004) Quantification of PDZ domain specificity, prediction of ligand affinity and rational design of super-binding peptides. *J. Mol. Biol.* **343,** 703–718